

## A Teleconnection Between Geopotential Height Anomalies over the North Atlantic and Precipitation in the Sahel Region of Africa

Daniel Barandiaran and Shih-Yu Wang

Department of Plants, Soils, and Climate, Utah State University, Logan, UT

### ABSTRACT

This study presents initial findings on a link between inter-annual variability in atmospheric circulations over the North Atlantic and precipitation over the African Sahel ( $P_S$ ). Our analysis shows that a meridionally stratified circulation wave train resembling the East Atlantic (EA) mode has a pronounced connection with  $P_S$ , and that the Climate Forecast System version 2 (CFSv2) fails to depict this EA mode and its  $P_S$  impact. Since the EA mode explains about 20% of variance of  $P_S$ , our analysis result is suggestive of a comparable portion of  $P_S$  variability that is missing in CFSv2 operational forecast.

### 1. Introduction

The African Sahel, a semi-arid region lying along the southern edge of the Sahara Desert, is characterized by large climate variability in summer precipitation on the inter-annual and inter-decadal time scales. The El Niño-Southern Oscillation (ENSO) is known as an important modulator of the Sahel summer precipitation ( $P_S$ ) (e.g., Joly and Voldoire, 2009). Other climatic forcing factors that modulate  $P_S$  include sea surface temperature (SST) anomalies in the Indian Ocean (Bader and Latif, 2003) and the tropical Atlantic (Brandt *et al.*, 2010). These previous findings were mainly based upon the concept of SST-driven, tropically confined teleconnections affecting  $P_S$ . By comparison, the process of a mid-latitude influence on the Sahel climate has drawn much less attention, possibly because of the prominent Sahara heat low and the robust mid-level African high (e.g., Chen 2005) potentially blocking any teleconnection influences originating from higher latitudes.

Most of the mid- to high-latitude climate oscillations, such as the North

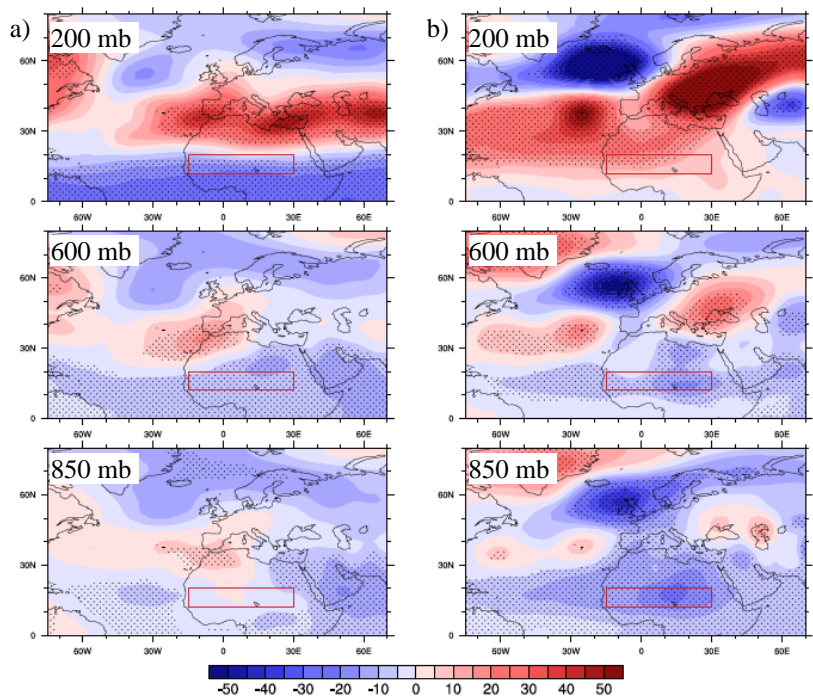


**Fig. 1** Composite differences of geopotential height over the years 1950-2010 for (a) La Niña summers (normalized Niño3.4 index < -1) minus El Niño summers (normalized Niño3.4 index > 1), and (b) wet summers (normalized  $P_S$  > 1) minus dry summers (normalized  $P_S$  < -1) during ENSO-Neutral years (normalized Niño3.4 index between -1 and 1). Precipitation data were obtained from the PREC/L. Red box indicates the Sahel region. Stippling indicates statistical significance of 95% per *t*-test.

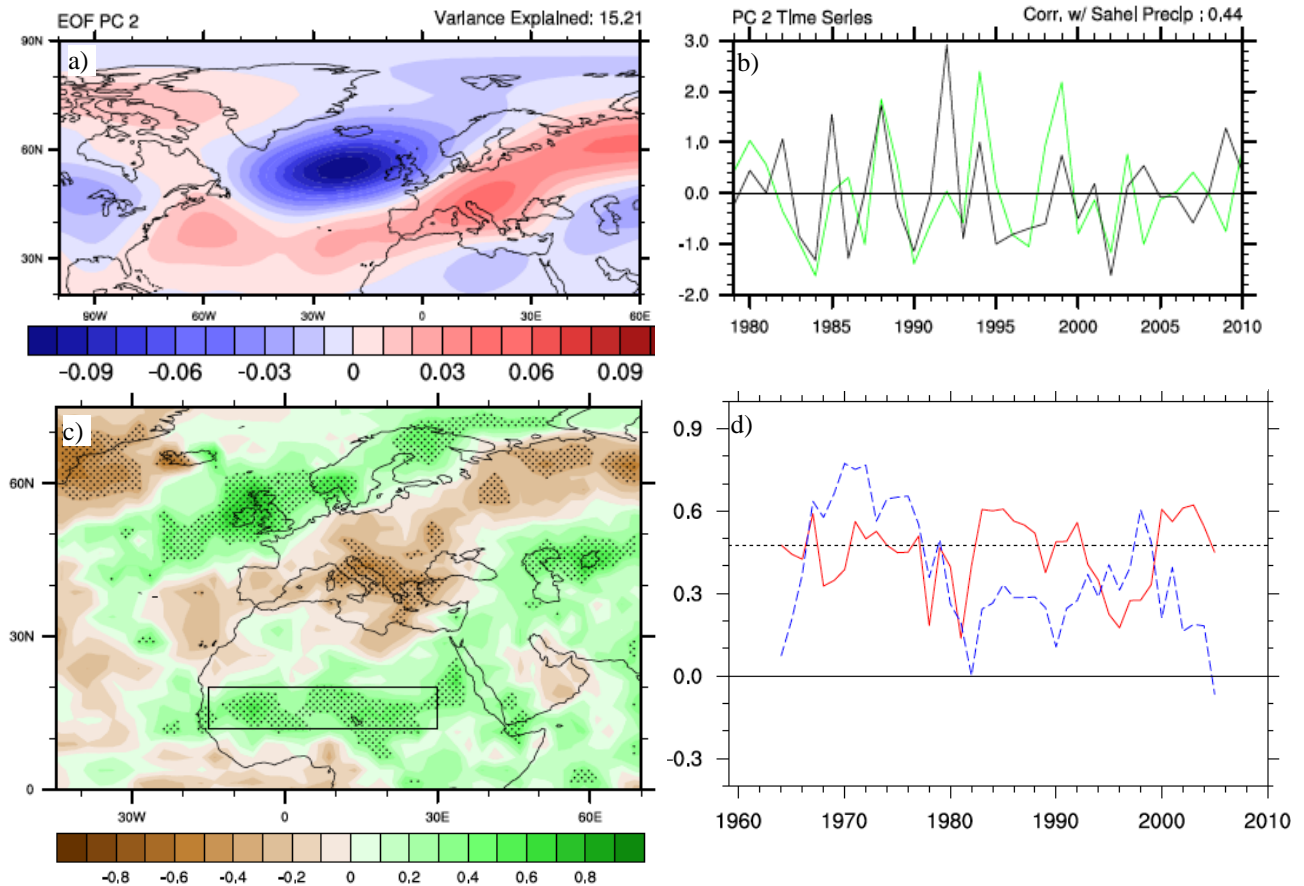


**Fig. 2** (a) Second EOF of the 600mb geopotential height during the JAS season over the years 1979-2010. (b) Normalized second PC time series (black) and the normalized JAS  $P_S$  (green). (c) One-point correlation map between PC2 time series and  $P_S$ ; stippling shows significance of 95% per t-test. (d) Sliding correlations of 11-year window between  $P_S$  and Nino-3.4 (red) and PC2 (blue); the horizontal dashed line indicates significance at 95%.

Atlantic Oscillation (NAO; Hurrell *et al.*, 2003), are predominately winter phenomena, even though their presence and effects during summer months have been studied (*e.g.*, Folland *et al.*, 2009). For the Sahel region, Chen and Wang (2007) noticed a connection between  $P_S$  and an atmospheric short-wave train in the North Atlantic during active ENSO years. In this study, we show a meridional wave train pattern that connects  $P_S$  with a possible higher latitude influence, regardless of the state of ENSO. Our analysis indicates that such a North Atlantic wave train is linked to the so-called East Atlantic (EA) mode, first identified by Barnston and Livezey (1987) as a center of anomalous 700mb geopotential height off the coast of Ireland with wave-like disturbances downstream across Europe. More importantly, we report that this EA- $P_S$  linkage is missing in one of the major climate forecast models, hence representing missing variability of  $P_S$  in seasonal climate prediction.

This study utilized the National Center for Environmental Prediction (NCEP)/National Corporation for Atmospheric Research (NCAR) Reanalysis I (Kalnay *et al.*, 1996) for atmospheric data. Rain gauge observations compiled and gridded by the National Oceanic and Atmospheric Administration (NOAA) precipitation reconstruction over land (PREC/L, Chen *et al.*, 2002) were used. We also analyzed the Global Precipitation Climatology Project (GPCP, Adler *et al.*, 2003), which synthesized rain gauge and satellite derived precipitation after 1979. The reforecast outputs (or hindcast) from the NCEP Climate Forecast System version 2 (CFSv2, Saha *et al.*, 2012) were examined for the forecast skill of  $P_S$ . Our primary focus is inter-annual variability after 1979; hence, all data after 1979 have been linearly detrended to remove long-term variability. Hereafter the term  $P_S$  and all other analyses are focused on the July-September (JAS) season.  $P_S$  was defined as the average precipitation within 12°-20° N and 15° W-30° E. Precipitation and various

climate indices used in the following analyses were normalized for ease of comparison between observational and model data.

## 2. The North Atlantic influence on $P_S$

### 2.1 Empirical evidence

The well-known ENSO influence on  $P_S$  is illustrated in Fig. 1a by the composites of geopotential height anomalies during ENSO-active years, *i.e.* La Nina minus El Nino years based on normalized JAS Nino-3.4 index less than -1/greater than 1. These composites reflect the resultant wet conditions in the Sahel. During ENSO-active years, the largest anomalies appear at 200mb over the Mediterranean Sea and North Africa, with considerably weaker amplitudes occurring at lower levels. During La Nina (El Nino) events, the circulation anomalies result in increased (decreased) strength of the tropical easterly jet (TEJ) and enhanced (suppressed) divergence aloft, which in turn enhances (suppresses) convection over the Sahel and West Africa (*e.g.*, Nicolson and Grist 2001). By comparison, the composite circulation anomalies between anomalous rainfall years (wet minus dry, using years when  $|\text{normalized } P_S| > 1$ , using PREC/L data), computed during ENSO-neutral years in which the absolute values of normalized Nino 3.4 index are less than 1, portray a quite different circulation pattern (Fig. 1b). First, substantial circulation anomalies leading to wet conditions in the Sahel (without the ENSO influence) are persistent throughout the lower troposphere. Second, there is a northwest-southeast oriented wave train extending from Greenland to North Africa, particularly at 600mb. The “center of action” of this wave train appears to be the pronounced negative anomaly west of Ireland

The meridional wave train pattern revealed in Fig. 1b is suggestive of a teleconnection influence emerging from higher latitudes on  $P_S$ . To examine the extent and origin of this wave train, we first conducted the Empirical Orthogonal Function (EOF) analysis on the 600mb geopotential height for the JAS seasons spanning 1979-2010 over the North Atlantic region as outlined in Fig. 2a. Shown in Fig. 2a is the second EOF that resembles the EA pattern (Barnston and Livezey 1987) as well as the composite wave train in Fig. 1b. This result is in agreement with the EOF leading modes of summertime sea level pressure by Folland *et al.* (2009); *i.e.* their EOF1 was the NAO and EOF2 was an EA-like pattern. What was not shown in Folland *et al.*'s analysis, however, is the significant correlation of the second principal component (PC2) with  $P_S$ , as is evidenced in Fig. 2b ( $r=0.43$ ). By contrast, the NAO (*i.e.* PC1) does not reveal any significant correlation with  $P_S$  ( $r = -0.07$ ).

Based upon their correlations during the period 1979-2010, ENSO explains 26% of the variance of  $P_S$  while PC2 explains 19%. Spatial correlations between PC2 and GPCP precipitation (Fig. 2c) show

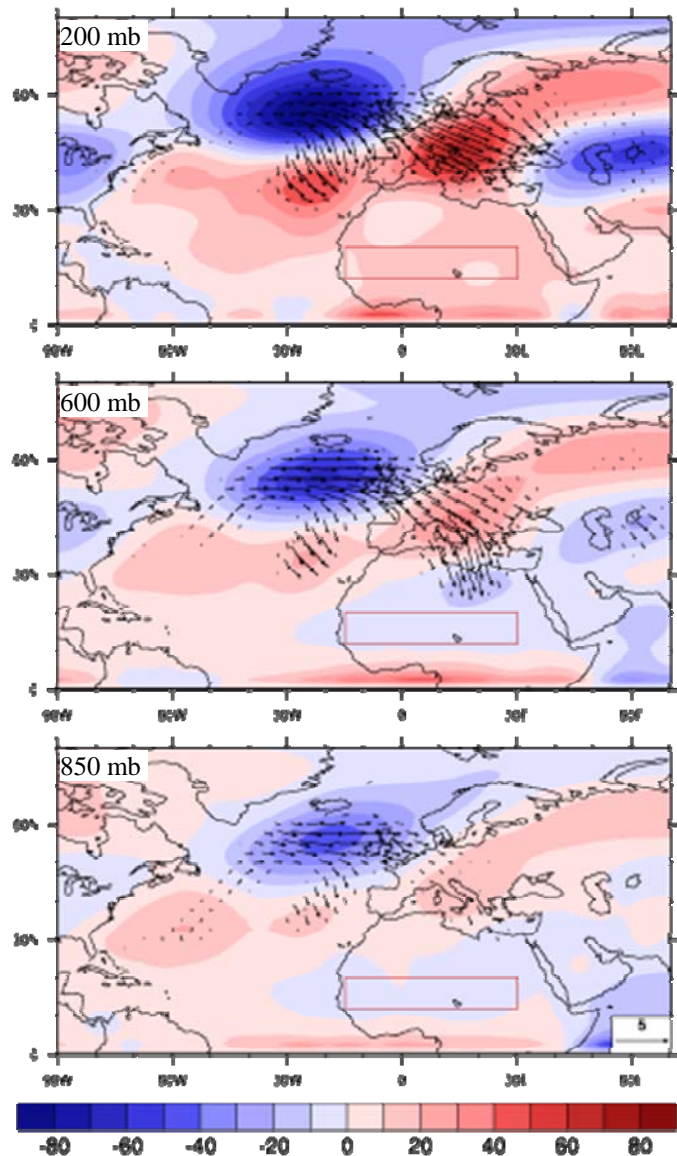


**Fig. 3** Same as Fig. 1b but for 1979-2010 and with the Rossby wave activity flux ( $W$ ) vectors. Vectors with the length smaller than  $1 \text{ m}^2 \text{ s}^{-2}$  were omitted.

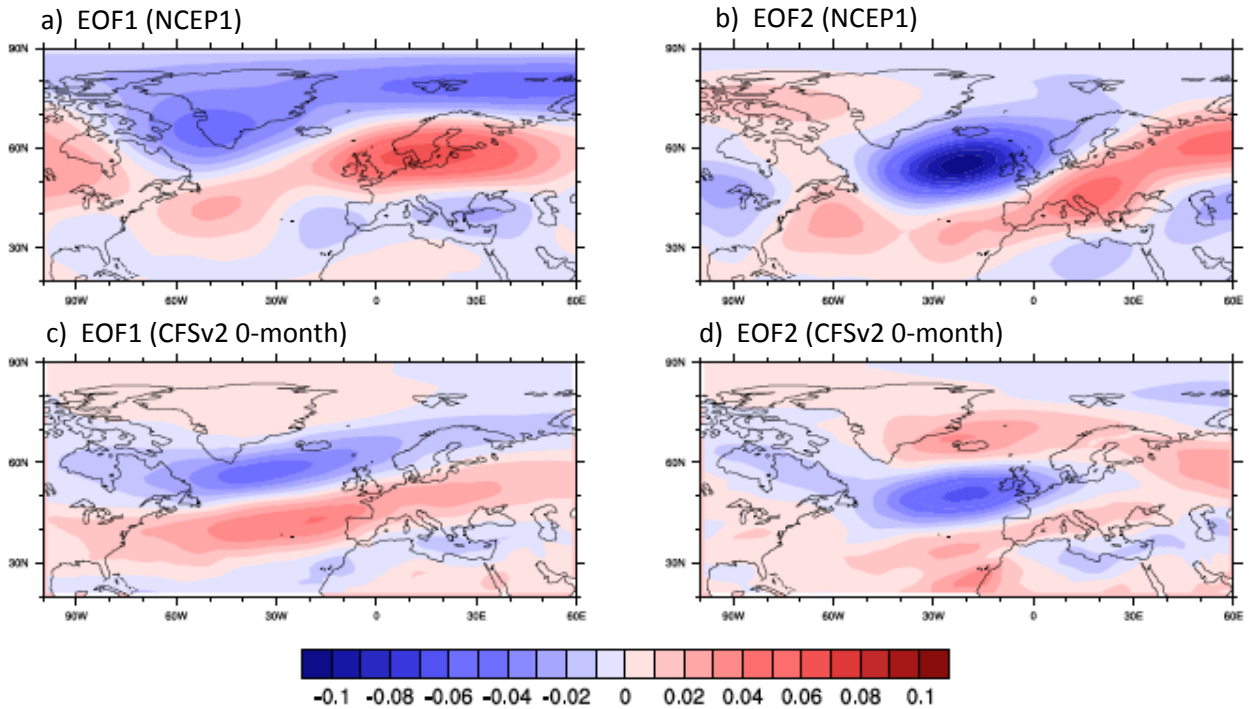


**Fig. 4** EOF analysis of the 600mb geopotential height of (a) EOF1 of NCEP1, (b) EOF2 of NCEP1, (c) EOF1 of CFSv2, and (d) EOF2 of CFSv2 at 0-month lead forecast.

significant responses across the Sahel region (boxed area). The precipitation correlations also reveal a north-south stratified structure that corresponds to the EOF2 (or EA) pattern. To examine the connection of PC2 with prominent climate modes, we computed the correlations of  $P_S$  with other common climate indices including ENSO, the Arctic Oscillation (AO), the Pacific-North American Pattern (PNA), the Atlantic Multidecadal Oscillation (AMO), and the Pacific Decadal Oscillation (PDO), obtained from the NOAA Climate Prediction Center (CPC; <http://www.cpc.ncep.noaa.gov/data/teledoc/>). The results showed that PC2 is independent of all these climate oscillations. Moreover, only ENSO and PC2 are significantly correlated with  $P_S$ .

According to Barnston and Livezey (1987) and the CPC, which provides the EA index (<http://www.cpc.ncep.noaa.gov/data/teledoc/ea.shtml>), the EA index was determined using the EOF analysis over the entire Northern Hemisphere (rather than the North Atlantic domain as in this study). Because EOF analysis is sensitive to geographic domain and dataset differences, a point-based EA index approach was utilized here. Based upon the EOF2 pattern as shown in Fig. 2a, we selected three geographical locations and applied the following formula:

$$EA = Z_{600}(5^{\circ}N, 15^{\circ}E) - 3 * Z_{600}(55^{\circ}N, 22.5^{\circ}W) + 2 * Z_{600}(30^{\circ}N, 20^{\circ}E), \quad (1)$$

where  $Z_{600}$  is the 600mb geopotential height in the JAS season. This point-based EA index correlates strongly with the PC2 time series ( $r=0.924$ ) and its spatial correlation with precipitation is essentially unchanged (not shown). Hereafter we refer to EA as the index built from Eq. (1), rather than PC2.

The relationship between  $P_S$  and EA was further examined by computing an 11 year sliding correlation, as shown in Fig. 2d by the center year. The linear trend within each 11-yr window was removed prior to computing the correlation to minimize the impact from inter-decadal variability. The sliding correlation of EA with  $P_S$  varies widely over time at roughly a 25 year timescale and has declined in the recent decade. The timing of this low-frequency variation does not correspond to that of either the AMO or the PDO. By comparison, the correlations between ENSO and  $P_S$  are relatively stable. A similar stabilization effect has been observed between ENSO and the all-India monsoon indices, in which the low-frequency fluctuations common in the sliding correlations between two random climatic time series are suppressed (Gershunov *et al.*

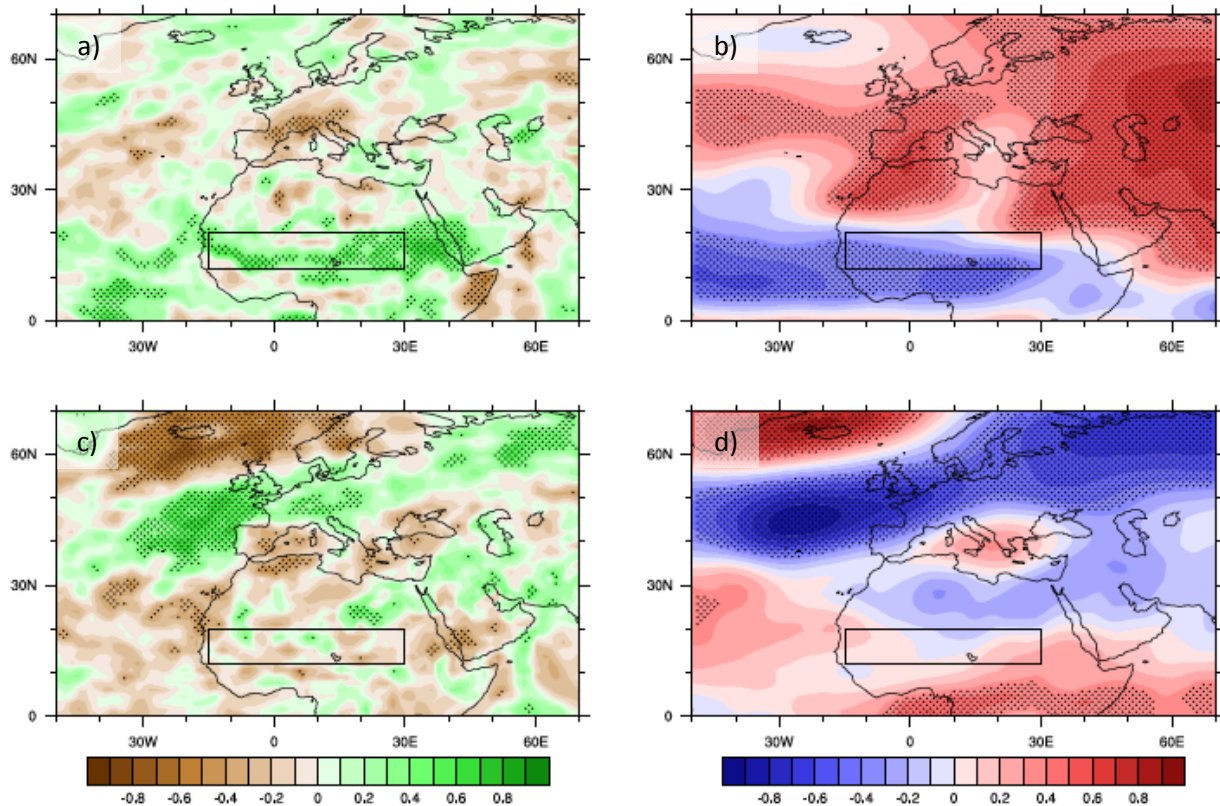


**Fig. 5** Spatial correlations of CFSv2 reforecasts (1982-2010) between (a) Nino3.4 index and precipitation, (b) Nino3.4 index and the 600mb geopotential height, (c) EA index and precipitation, and (d) EA index and geopotential height. Stippling shows statistical significance of 95% per r-test. Box shows the Sahel region.

2001). At this point we do not have evidence to rule out the possibility that the fluctuating EA- $P_s$  correlations are stochastic noise, and not a realization of multidecadal modulations.

## 2.2 Dynamical inference

Having established an empirical connection between EA and  $P_s$ , we next explored the dynamic mechanism of this connection by analyzing the horizontal-component Rossby wave-activity flux ( $W$ , derived per Takaya and Nakamura, 2001) during EA-active years (*i.e.*  $|EA| > 1$ ). This  $W$  vector provides a measure of propagation of Rossby wave energy and enstrophy. Calculation of this wave-activity flux is not dependent on spatial or temporal averaging and therefore is suitable for any particular time period (see Takaya and Nakamura, 2001 for details).

As shown in Fig. 3, *i.e.* the wet-dry composite during ENSO neutral years, the wave-activity flux at the upper troposphere (top panel) is mainly zonal in direction and confined to north of  $30^\circ$  N. In the middle troposphere however (middle panel), there is a strong wave-activity flux penetrating into North Africa, moving along the downstream portion of the wave train over the Mediterranean Sea. At lower troposphere (bottom panel), the wave-activity flux crosses the Mediterranean into North Africa but does not extend as far inland as at 600mb. This  $W$  propagation is consistent with the EA composite (not shown) and is suggestive of the forcing mechanism leading to the middle and lower tropospheric circulation patterns associated with the Sahelian wet/dry anomalies (Fig. 1b).

The rather large wave-activity flux over North Africa at 600mb has an implication for regional circulation anomalies. It appears that the mid-level anticyclone that stations itself over the Sahara Desert can be modulated by teleconnection emanating from higher latitudes. This teleconnection may affect the position and/or intensity of the African easterly jet (AEJ) which, in turn, regulates the activity of African easterly

waves (AEWs) (Chen, 2006). Since AEWs form at both sides of the AEJ core (Chen 2006) it is possible that this injection of Rossby wave-activity energy modulates the middle-level anticyclone and the AEJ, as well as the development of these AEWs, thereby influencing  $P_S$ . Further investigation is needed for the dynamic processes of this documented EA- $P_S$  teleconnection.

### 3. Forecast skill for EA

An important question derived from the aforementioned finding of the EA- $P_S$  connection lies in its depiction in climate prediction, that is, how well do operational climate forecast models capture EA and its impact on  $P_S$ ? Here we tested hindcast output from CFSv2 to evaluate the model's performance. Following the observational analysis in Fig. 2, we first conducted an EOF analysis on the 600mb geopotential height of CFSv2 at zero-month lead time. The loading patterns and time series for the EOFs were substantially different from those of the NCEP reanalysis data (Fig. 4a-b). Both EOF 1 and 2 (Fig. 4c-d) of CFSv2 exhibit a distinct zonal loading pattern, with considerably smaller magnitude and a north-south – rather than northwest-southeast – orientation as in the reanalysis data. CFSv2 apparently does not reproduce the EA, signified by the very low temporal correlation of -0.16 at 0-month forecast and essentially no correlation at 3-month forecast ( $r=0.01$ ). Apparently, the EOF approach to define EA as was used in Barnston and Livezey (1987) and the CPC is not suitable for the analysis of CFSv2 outputs, hence justifying the use of the point-based EA index.

In terms of ENSO, the CFSv2 performs well in reproducing the Nino-3.4 index ( $r=0.97$ ) and reasonably captures  $P_S$  ( $r=0.78$ ) at 0-month forecast. At forecast month 3, CFSv2 still has a robust correlation of 0.81 for Nino-3.4, but the correlation of  $P_S$  forecast drops to 0.33. When we consider spatial correlations between modeled ENSO/EA and  $P_S$  in CFSv2 at 0-month lead forecast (Fig. 5a/c),  $P_S$  responds as expected to modeled ENSO forcing. However, there is essentially no connection between forecast precipitation and forecast EA in the Sahel. Spatial correlation with the 600mb streamfunction (Fig. 5b,d) shows that modeled circulation response to ENSO forcing is a reasonable approximation to that of observational data (Fig 1a), but the EA wave pattern does not reveal the same sign of circulation anomalies over North Africa, hence the insignificant precipitation response in CFSv2 (Fig. 5c).

### 4. Summary

CFSv2 has been improved in terms of forecasting ENSO, particularly SST evolutions in the Nino 3.4 region (*e.g.*, Wu *et al.* 2009). This is a promising step in forecasting the well-established connection between ENSO and  $P_S$ . Correspondingly, modeled  $P_S$  responds appropriately to ENSO forcing through the first few forecast months. However, there is a discrepancy in the variability of atmospheric circulations in the North Atlantic and North Africa between CFSv2 and observational data, in that EA is not captured at all even at 0-month forecast. Therefore, an important portion (~20%) of the  $P_S$  variance will be missing in CFSv2 forecasts. Since EA is predominately a winter mode (whereas this study only considers the summer season), an examination of model performance in atmospheric variability during the winter season could help to determine if this deficiency of forecasting EA is seasonal in nature, or is intrinsic to CFSv2 regardless of season.

In addition to its known connection with ENSO,  $P_S$  is significantly and positively correlated with EA. During the positive phase of EA, transport of Rossby wave activity brings energy from the mid-latitudes into North Africa at the middle troposphere where the core of the AEJ is located. CFSv2 fails to capture this higher-latitude variability mode, but forecasts reasonably the state of ENSO and the associated Sahel precipitation anomalies up to 3 months. In future work we will further explore the dynamical implications for the connection between  $P_S$  and this atmospheric/EA mode. We will also seek an explanation for the multidecadal fluctuations of EA's influence on  $P_S$ .

### References

- Adler, R. F., and Co-authors, 2003: The version-2 Global Precipitation Climatology Project (GPCP) monthly precipitation analysis (1979-present). *J. Hydrometeor.*, **4**, 1147-1167. doi: 10.1175/1525-7541(2003)004<1147:TVGPCP>2.0.CO;2.

- Bader, J., M. Latif, 2003: The impact of decadal-scale Indian Ocean sea surface temperature anomalies on Sahelian rainfall and the North Atlantic Oscillation. *Geophys. Res. Lett.*, **30**, 2169. doi: 10.1029/2003GL018426.
- Barnston, A. G., and R. E. Livezey, 1987: Classification, seasonality and persistence of low-frequency atmospheric circulation patterns. *Mon. Wea. Rev.*, **115**, 1083-1126. DOI: 10.1175/1520-0493(1987)115<1083:CSAPOL>2.0.CO;2.
- Brandt, P., G. Caniaux, B. Bourles, A. Lazar, M. Dengler, A. Funk, V. Hormann, H. Giordani, and F. Marin, 2010: Equatorial upper-ocean dynamics and their interaction with the West African monsoon. *Atmos. Sci. Lett.*, **12**, 24-30. DOI: 10.1002/asl.287.
- Chen, M. P.-P. Xie, J. E. Janowiak, and P. A. Arkin: 2002: Global land precipitation: a 50-yr monthly analysis based on gauge observations. *J. Hydrometeor.*, **3**, 249-266. doi: 10.1175/1525-7541(2002)003<0249:GLPAYM>2.0.CO;2.
- Chen, T.-C., 2005: Maintenance of the midtropospheric North African summer circulation: Saharan high and African easterly jet. *J. Climate*, **18**, 2943-2962. doi: 10.1175/JCLI3466.1.
- , 2006: Characteristics of African easterly waves depicted by ECMWF reanalyses for 1991-2000. *Mon. Wea. Rev.*, **134**, 3539-3566. doi: 10.1175/MWR3529.1.
- , and S.-Y. Wang, 2007: Interannual variation of the Sahel rainfall. *Geophys. Res. Abs.*, **9**, 11206. SRef-ID: 1607-7962/gra/EGU2007-A-11206.
- Folland, C. K., J. Knight, H. W. Linderholm, D. Fereday, S. Ineson, and J. W. Hurrell, 2009: The summer North Atlantic Oscillation: past, present, and future. *J. Climate*, **22**, 1082-1103. DOI: 10.1175/2008JCLI2459.1.
- Gershunov, A., N. Schneider, and T. Barnett, 2001: Low-frequency modulation of the ENSO-Indian monsoon rainfall relationship: signal or noise? *J. Climate*, **14**, 2486-2492. DOI: 10.1175/1520-0442(2001)014<2486:LFMOTE>2.0.CO;2.
- Hurrell, J. W., Y. Kushnir, G. Ottersen, and M. Visbeck, 2003: The North Atlantic Oscillation: Climatic significance and environmental impact. *Geophys. Monogr. Series*, **134**, 279 pp. ISBN: 0-87590-994-9.
- Joly, M., and A. Voltaire, 2009: Influence of ENSO on the West African monsoon: temporal aspects and atmospheric processes. *J. Climate*, **22**, 3193-3210. doi: 10.1175/2008JCLI2450.1.
- Kalnay, E., and Co-authors, 1996: The NCEP/NCAR 40-year reanalysis project. *Bull. Amer. Meteor. Soc.*, **77**, 437-472. doi: 10.1175/1520-0477(1996)077<0437:TNYRP>2.0.CO;2.
- Nicholson, S. E., and J. P. Grist, 2001: A conceptual model for understanding rainfall variability in the West African Sahel on interannual and interdecadal timescales. *Int. J. Climatol.*, **21**, 1733-1757.
- Saha, S. S., and Co-authors, 2012: The NCEP Climate Forecast System version 2. *J. Climate* (submitted).
- Takaya, K., and H. Nakamura, 2001: A formulation of a phase-independent wave-activity flux for stationary and migratory quasigeostrophic eddies on a zonally varying basic flow. *J. Atmos. Sci.*, **58**, 608-627. doi: 10.1175/1520-0469(2001)058<0608:AFOAPI>2.0.CO;2.
- Wu, R., B. P. Kirtman, H. van den Dool. 2009. An analysis of ENSO prediction skill in the CFS retrospective forecasts. *J. Climate*, **22**, 1801-1818. doi: 10.1175/2008JCLI2565.1.